Stanford Exploration Project, Report 95, October 10, 1997, pages 1–219

Stanford Exploration Project, Report 95, October 10, 1997, pages 1–219

Seismic Anisotropy in Trinidad: More parameter estimation

Tariq Alkhalifah and Dave Rampton[1]

keywords: *anisotropy, parameter estimation, interpretation*

ABSTRACT

New estimates of anisotropy have revealed more details of the subsurface in Trinidad. These estimates are obtained by including more realistic constraints on the anisotropic inversion, which eventually helped boost the stability of the process. The anisotropic parameter η, which, if not zero, implies the existence of anisotropy, is used to discriminate conservatively between shales and sands. The underlying theory is that shales induce anisotropy, positive η in particular, and sands do not. The η estimates, through have nice lateral correlation, react to the presence of faults. Correlation of these η results with gamma-ray well-log measurements used as a shale estimate proves the credibility of the results. This finding confirms the hypothesis that anisotropy is caused by shales in the subsurface, and, consequently, we can use the inversion for interval η to estimate lithology.

INTRODUCTION

The discrimination between shales and sands in the subsurface is key to oil exploration. Reservoirs usually exist in sand layers, sandwiched between large columns of shale layers. In a previous paper (Alkhalifah and Rampton, 1997), we showed that the anisotropy parameter η, extracted from surface seismic P-wave data, can be used, in a low resolution sense, to discriminate between shale-dominated layers and sand-dominated ones. The underlying theory is that shales induce anisotropy (Banik, 1984), positive η in particular, and sands do not ($\eta \approx 0$). In our earlier paper (Alkhalifah and Rampton, 1997), we implemented the nonhyperbolic moveout inversion of Alkhalifah (1997) on a line that included spread length with offsets up to 6 km. The resulting η estimates showed reasonable correlations with the reflections on seismic sections. Also, the estimates correlate well with gamma-ray well-log measurements, used as a shale estimate, which proves the credibility of these results.

[1]**email:** tariq@sep.stanford.edu,dcrampton@amoco.com

In this paper, we use modified inversion tools, compared to the one used in our previous paper (Alkhalifah and Rampton, 1997), which although are based on the same underlying theory of nonhyperbolic inversion, provide more stable estimates of η over a larger scale. The inversion now includes a damping process that constrains the η values at depth, where the inversion is less stable, and a picking feature that helps constrain the NMO velocity and thus avoid multiples. We apply the inversion to two portions of a line from Trinidad and obtain 2-D plots of η distribution in the subsurface at these two regions.

THEORY

Alkhalifah and Tsvankin (1995) demonstrated that, for transversely isotropic (TI) media with a vertical symmetry axis (VTI media), just two parameters are sufficient for performing all time-related processing, such as NMO correction (including nonhyperbolic moveout correction, if necessary), DMO correction, and prestack and poststack time migration. One of these two parameters, η, is a dimensionless parameter, whose departure from zero implies anisotropy, and the other, V_{nmo}, is the short-spread normal moveout (NMO) velocity for horizontal reflectors. These two parameters can be obtained solely from surface seismic P-wave data, using estimates of stacking velocity for reflections from interfaces having two distinct dips (Alkhalifah and Tsvankin, 1995). VTI media induce nonhyperbolic moveout of reflections that depends on V_{nmo} and η at large offsets. Alkhalifah (1997) showed that these two parameters can be obtained by analyzing the moveout at far offsets. The direct output from such an inversion (or velocity analysis) is the effective values of V_{nmo} and η, which include the combined (average) influence of the overburden. These effective values are converted to interval values using layer-stripping equations. Interval η estimates resulting from the inversion are a direct low-resolution indicator of lithology, in which low η values indicate sand-dominated intervals, and positive η values indicate shale-dominated intervals.

THE TRINIDAD DATA

The line acquired from the Trinidad region contains data with offsets that extend to 6 km. This 2-D line was acquired in the regional subsurface dip direction. The source-to-receiver spacing ratio is three, and the maximum fold in the data is 90. Because of the large size of offsets acquired, a nonhyperbolic inversion (Alkhalifah, 1997) was used on these data. Also, many wells exist along this line; one near CMP location 1100 and another near CMP 1220, see Figure 4. The gamma-ray measurements from these wells are reliable shale-sand discriminators, and thus can be used to calibrate our results. In a previous paper (Alkhalifah and Rampton, 1997), we showed some sparse η estimates from this line. In this study, we have obtained more detailed estimates of η in the same region, as well as included detailed estimates from another part of the line, not shown in the earlier paper.

PARAMETER ESTIMATION

We use the nonhyperbolic moveout inversion of Alkhalifah (1997) to estimate interval η for the seismic line from Trinidad. The result of this inversion is an interval η curve as a function of time. This inversion, though based on a laterally homogeneous medium assumption, has some tolerance to lateral inhomogeneity, such as the lateral inhomogeneity associated with most faults.

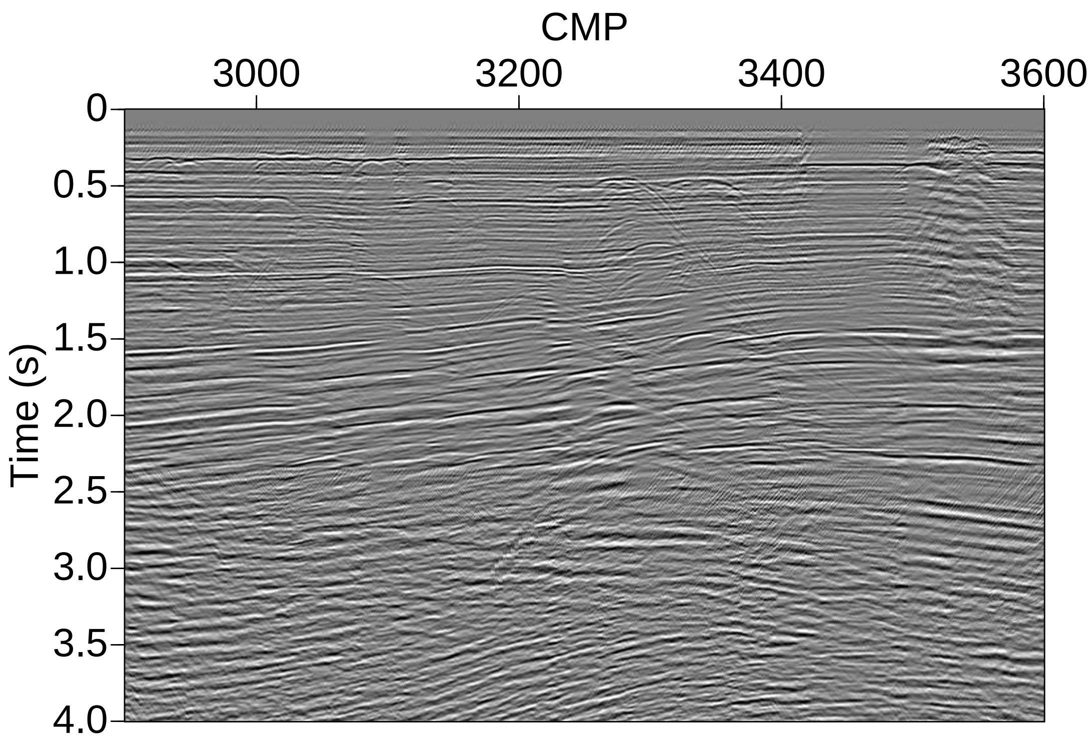

Figure 1: A stacked section of the line from offshore Trinidad, after applying NMO and isotropic homogeneous DMO. The NMO correction is based on the velocities provided by Amoco. tariq4-dmois [NR]

Figure 1 shows a zero-offset section that contains a large number of faults. Note that the data beyond 2.5 s are of poor quality.

Figure 2 shows five η curves superimposed on a migrated section from this region. Specifically, the zero η value at the top of each curve is placed at the position of the measurement corresponding to that curve. The lateral correlation, especially up shallow, between these curves, which are nearly 1.25 km apart, is notable. The difference between the curves at depth is a result of the complexity of the medium at depth. We can attribute some of these differences to the limitations of this inversion at later times (Alkhalifah, 1997).

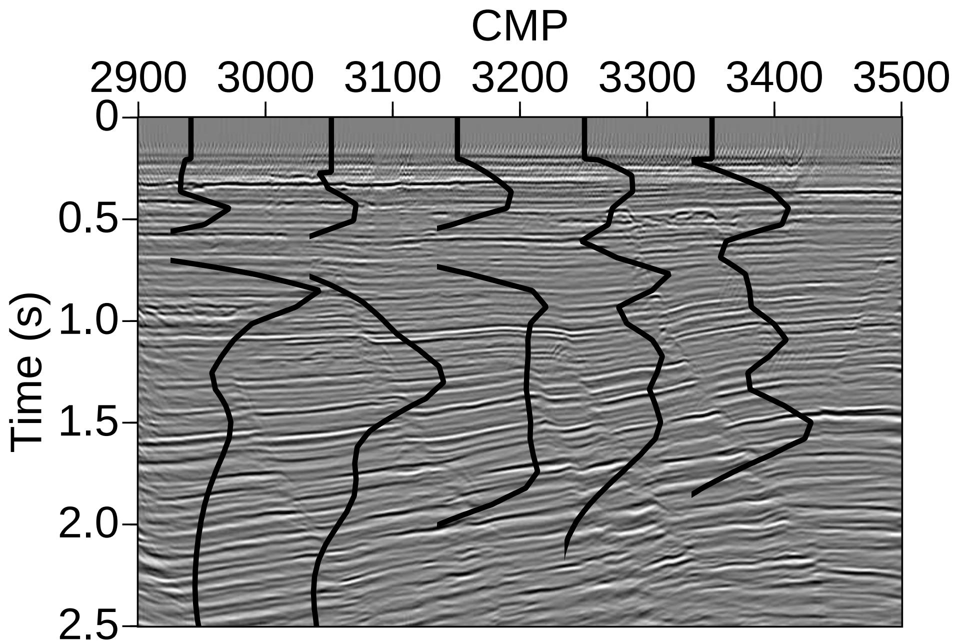

Figure 2: Five interval η curves superimposed on a time-migrated section. These η values are placed in their accurate location on the migrated image. The plot range for each curve is between -0.01 and 0.24. tariq4-migcurv2900-3500f [NR]

A more laterally continuous representation is given by the 2-D plot of interval η in Figure 3 (at the bottom), where measurements were taken at practically every CMP location and subsequently used to estimate a more continuous interval η distribution. Figure 3 (at the top) shows the interval velocity extracted through the same process. Most of the observations obtained from Figure 2 apply to Figure 3 as well. Moreover, the correlation between the layering and the η distribution is even more apparent in Figure 3. Faults probably explain the sudden variations of η at certain locations. Overall, however, η has good lateral continuity. Some faulting has disrupted this continuity, and these faults are indicated in gray. The lack of information beyond 2.0 s is a result of the methods depth limitation and the poor data quality at depth. Also, data at CMP locations 3450-3600 are of low quality, because of the presence of shallow gas in the area. Some of the effect of the shallow gas can be seen on the stacked section in Figure 1. The estimates in Figure 3 are of low resolution both laterally and vertically, and as a result no abrupt fault affects are apparent. Nevertheless, there is some vertical shift in the η distribution between the sides of some of the large faults.

Figure 4 shows a zero-offset section that also contains a large number of faults. Wells are located at CMP 1100 and 1220; both above an anticline structure. Overall, this area has the same characteristics as the area depicted in Figure 1 despite the large distance between the two regions ($\approx$ 25 km).

Figure 5 shows seven η curves superimposed on a migrated section from this region. These η curves are placed in their respective positions in Figure 5. The lateral correlation between these curves, which are about 1.25 km apart, is also remarkable. Especially remarkable is the correlation between the thickness of the shale layers and the size of η as we can see by comparing the measurements at CMP 750 with that at CMP 1050 for the top layer. These η values are plausible, especially compared with the large η values we obtained for our earlier paper. Part of the reason for this improvement is the improved stability measures applied to the new estimates.

A more continuous estimation of η is given by the 2-D plot of η in Figure 6 (at the bottom), which resembles Figure 3. Figure 6 (at the top) also shows the interval velocity extracted through the same process. Again, most of the observations regarding Figure 5 apply here as well. However, more detail is apparent in this continuous η representation. The three major faults in the area are drawn to show their effect on the measurements. Again, the poor quality of data at later times is the reason behind the lack of estimates at depth. Figure 7 shows a sample CMP gather (CMP 1000) after NMO correction. Probably, the last laterally-continues reflection appears just above the 2-second mark.

Figure 8 shows a crude lithologic interpretation estimated solely from the anisotropic inversion. The interpretation is based on the fact that shales are anisotropic, and therefore exhibit large positive η values, while sands are essentially isotropic with near-zero values of η. The second sand layer may also include a lot of shales because the drop in η is not very definite. Also, at this depth the data quality is bad.

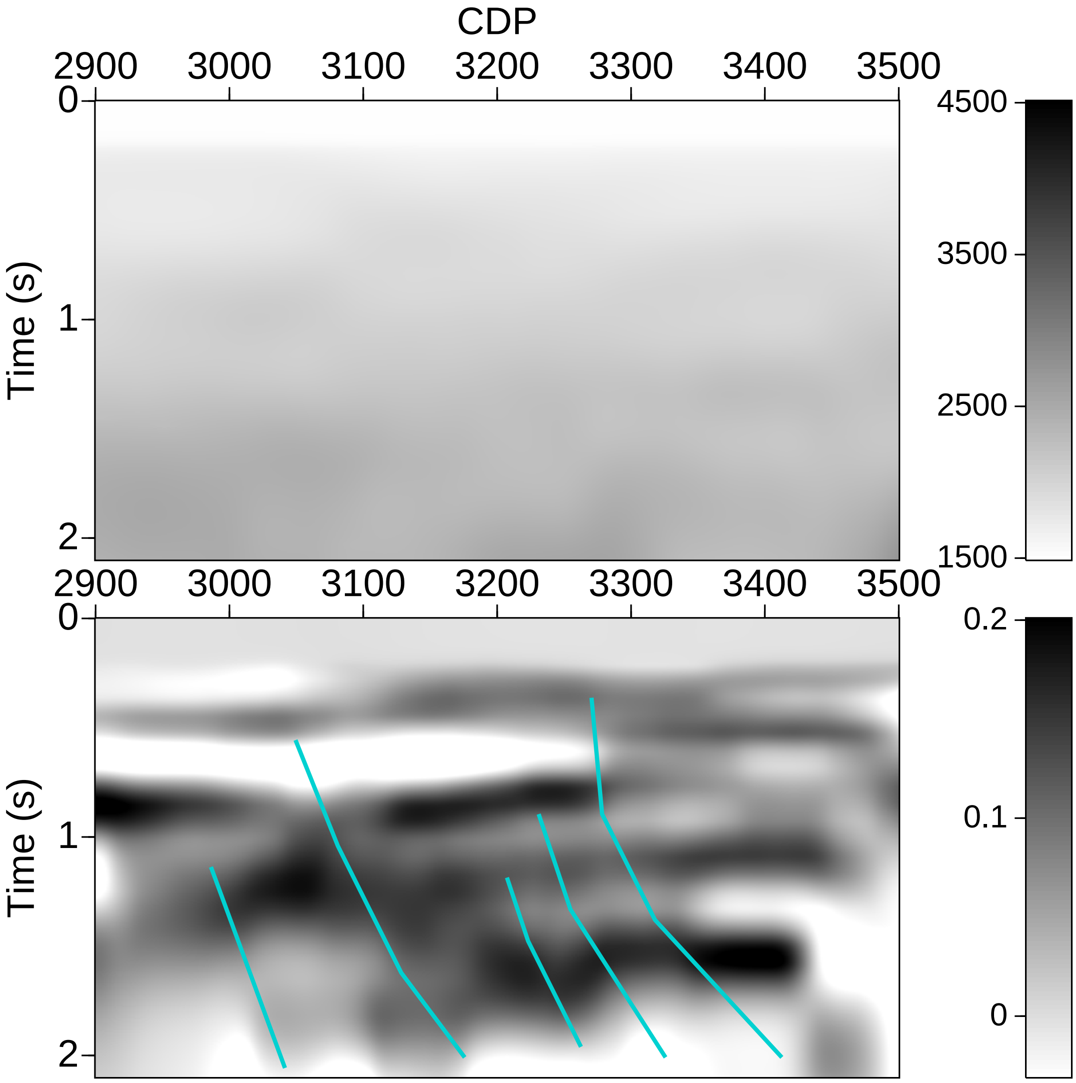

Figure 3: Top: the interval NMO velocity corresponding to the data in Figure 1. Bottom: the interval η values for the same data. The gray lines correspond to some interpreted faults in the area. tariq4-fault2900-3500 [NR]

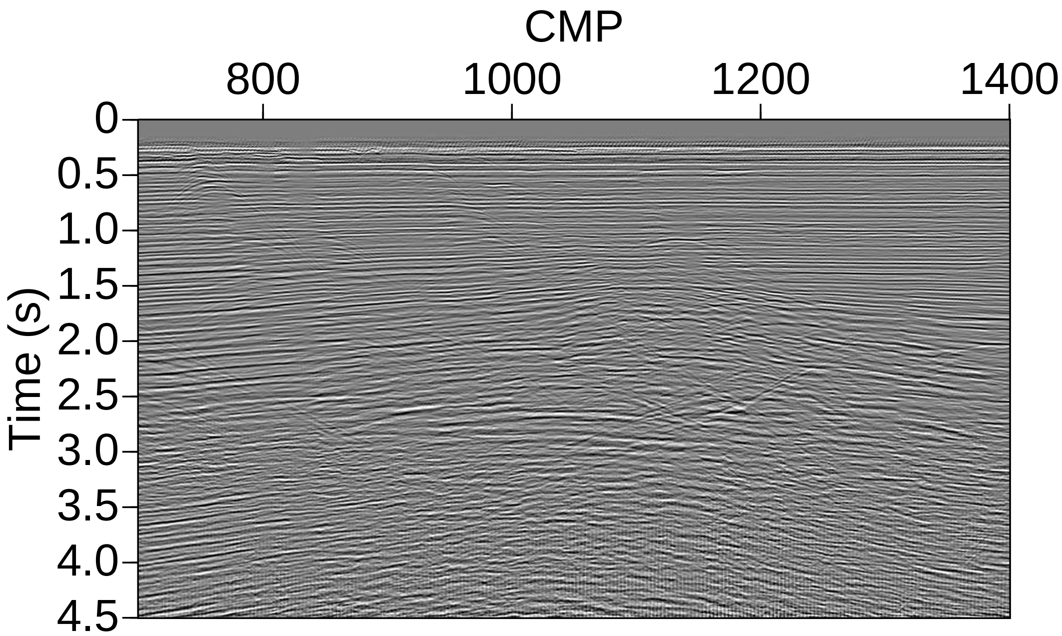

Figure 4: Stacked section of another part of the line from offshore Trinidad, after applying NMO and isotropic homogeneous DMO. The NMO correction is based on the velocities provided by Amoco. tariq4-stack700-1400 [NR]

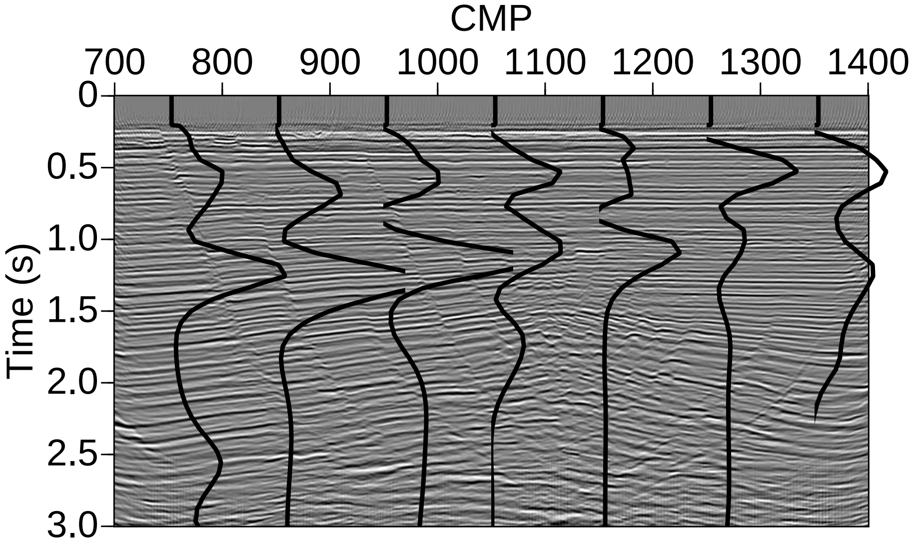

Figure 5: Seven interval η curves superimposed on the time-migrated section. These η values are placed in their accurate location on the migrated image. The plot range for each curve is between -0.01 and 0.24. tariq4-migcurvfff [NR]

WELL CONTROL

To verify the preceding observations, Figure 9 and 10 compares the η curves with gamma ray logs available from nearby wells. Two locations are shown, one at CMP 1100, another, close by, at CMP 1220. At both locations, the Gamma ray logs indicate the presence of sands just prior to the one second mark. At this time, the η curve also shows small values suggesting the this part of the vertical column is isotropic. Because shales induce anisotropy, more likely than not, this part of the section corresponds to sands. Figure 6 provides information from seismic data of the lateral extent of this sand layer, or layers. At CMP locations 1100 and 1220, the correlation between the well-log measurements, at a lower resolution, and the η curve is remarkable. Recall, that the η curve is obtained in its entirety from P-wave surface seismic data. Yet, information like the low frequency character of the shale-sand content is extracted from these data.

CONCLUSION

By acknowledging the influence of anisotropy on seismic data, we have roughly estimated the anisotropic parameter η. This parameter, if accurately estimated, can

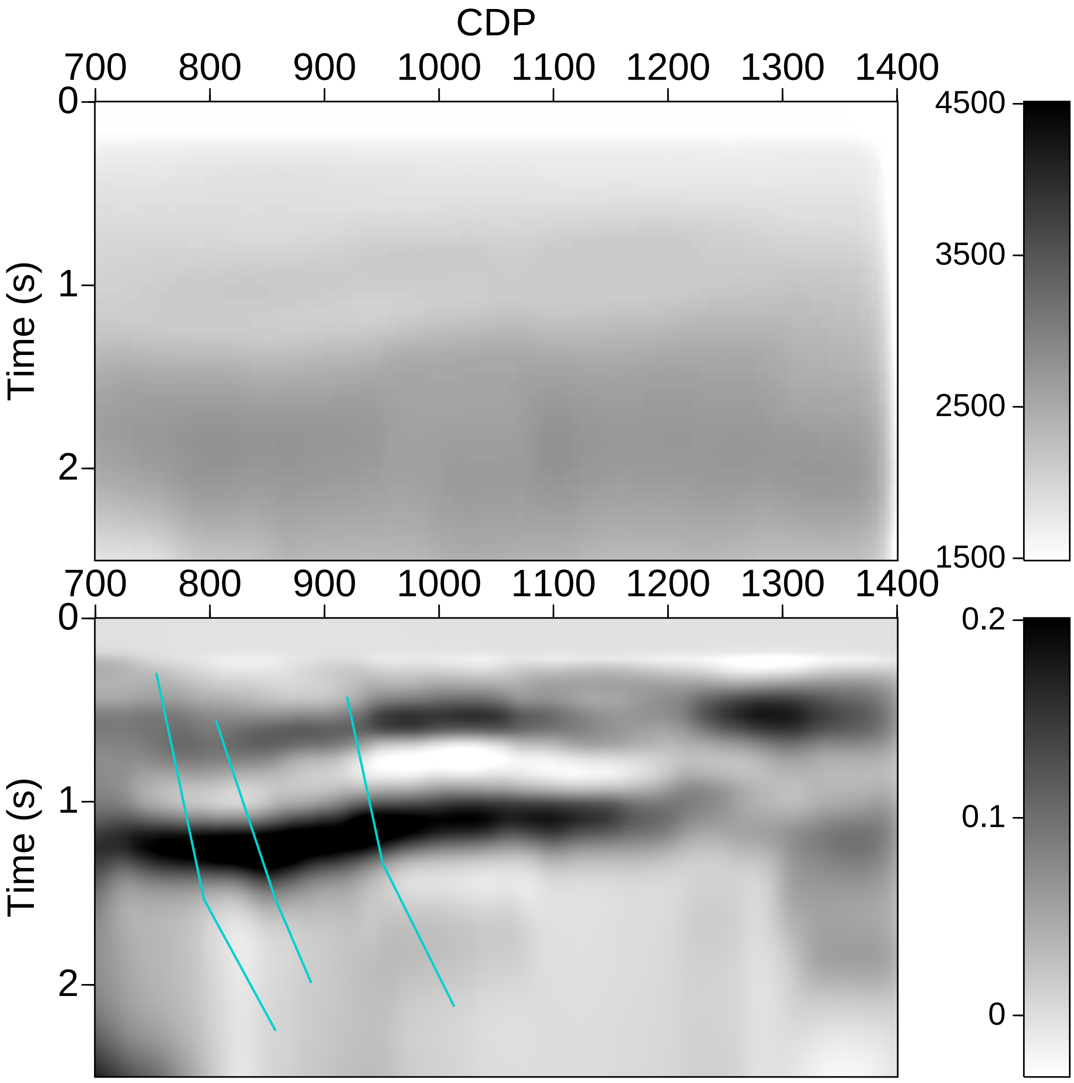

Figure 6: Top: the interval NMO velocity corresponding to the data in Figure 4. Bottom: interval η values for the same data. tariq4-fault700-1400 [NR]

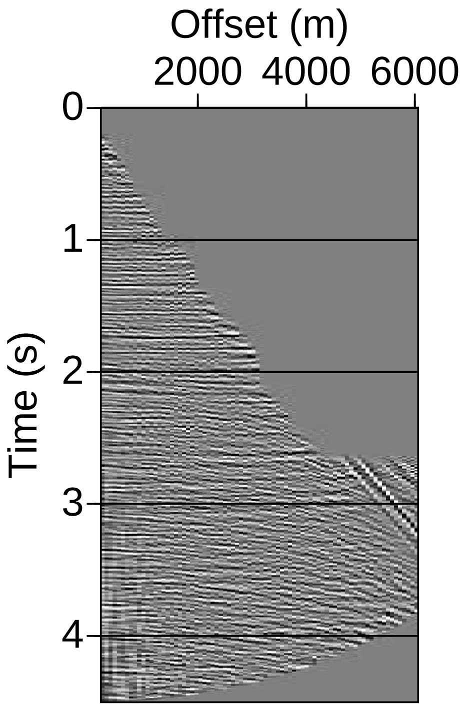

Figure 7: Common-midpoint gather (CMP) 1000 after NMO correction with the proper NMO velocity obtained from conventional velocity analysis. tariq4-cmp1000 [NR]

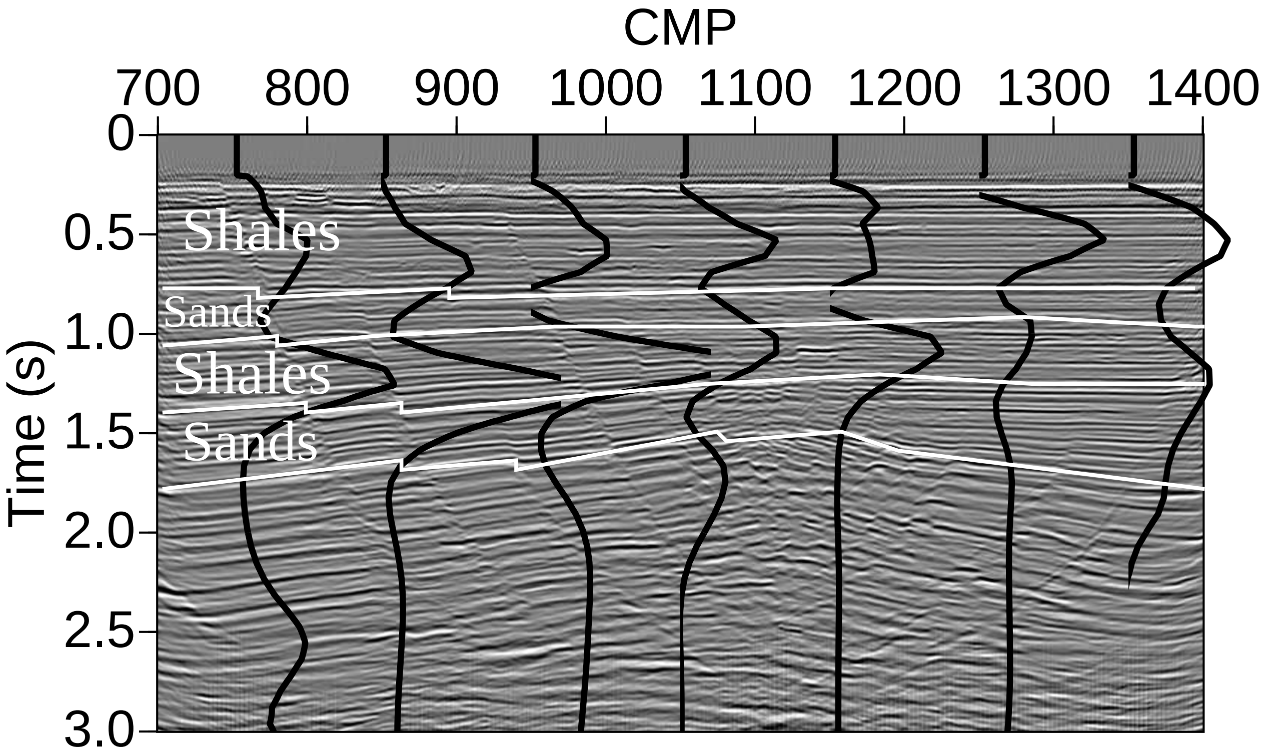

Figure 8: A lithological interpretation of the sand and shale content of the surface as estimated by the interval η values obtained from the inversion. The white lateral lines follow seismic reflections. The second sand layer may include respectable amounts of shale. tariq4-intersand [NR]

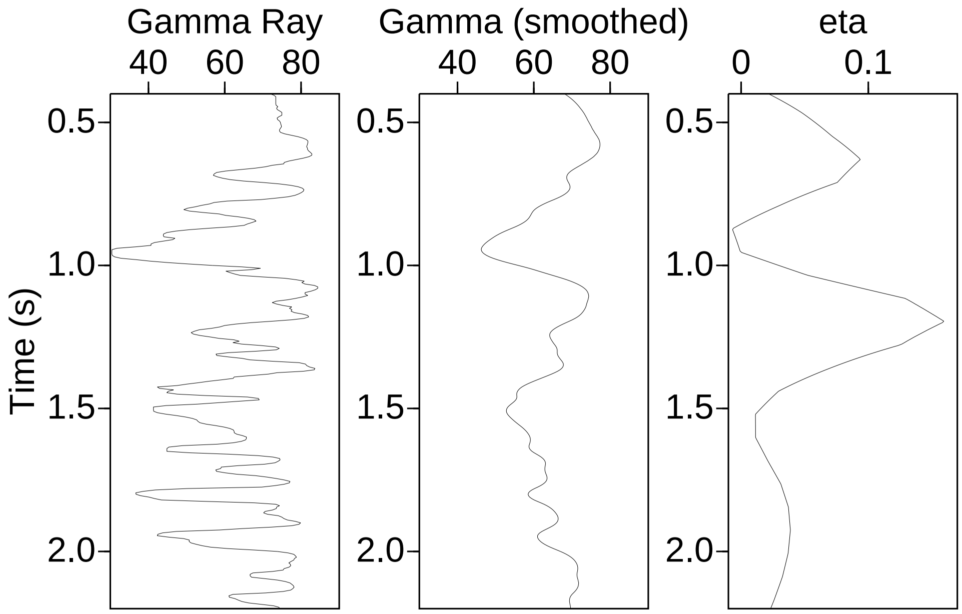

Figure 9: Left: Gamma ray logs from a well located at CMP location 1100 in Figure 4. Middle: A smoothed version of the Gamma ray measurements using a conventional box function smoother with a window 0.1 second. Right: interval η values obtained from the seismic data for the same location. tariq4-data7-gamma.well.plot [NR]

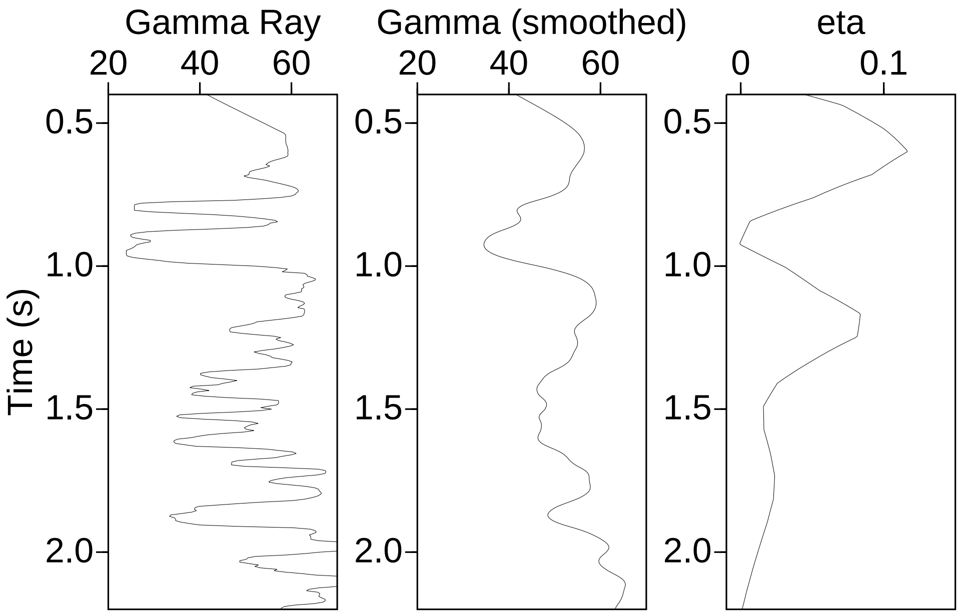

Figure 10: Same as Figure 9, but for CMP location 1220. Left: Gamma ray measurements. Middle: A smoothed version of the Gamma ray measurements using a conventional box function smoother with a window 0.1 seconds. Right: interval η values obtained from the seismic data for the same location. tariq4-data2-gamma.well.plot [NR]

be used to discriminate between shales and sands in the subsurface. Obtaining such information from surface seismic P-wave data has important implications for deep water surveys, where the cost of drilling wells is large. This technique does not require expensive or unusual acquisition procedures—the only requirement is a new look at existing data using refined processing techniques that incorporate real geologic parameters.

REFERENCES

Alkhalifah, T., 1997, Velocity analysis using non-hyperbolic moveout in transversely isotropic media: Geophysics, in press.

Alkhalifah, T., and Tsvankin, I., 1995, Velocity analysis for transversely isotropic media: Geophysics, **60**, 1550-1566.

Alkhalifah, T., and Rampton, D., 1997, Seismic Anisotropy in Trinidad: Processing and interpretation: SEP-94, 299-325.

Banik, N. C., 1984, Velocity anisotropy of shales and depth estimation in the North Sea basin: Geophysics, **49**, 1411–1419.

Thomsen, L., 1986, Weak elastic anisotropy: Geophysics, **51**, 1954–1966